ansa-Ferrocenes with both Trisulfide and Hydrocarbon Straps

Paul F. Brandt

*Department of Chemistry and Physics, Western Carolina University,
Cullowhee, North Carolina 28723*

David L. Compton and Thomas B. Rauchfuss*

*School of Chemical Sciences, University of Illinois at Urbana Champaign,
Urbana, Illinois 61801*

Received January 2, 1998

Described are two new ferrocenes, each containing two different straps linking the pair of cyclopentadienyl rings. The first, $Fe(C_5H_3)_2$-1,1′-S_3-3,3′-C_2Me_4, was characterized by single-crystal X-ray diffraction and shown by ^1H NMR studies to consist of two slowly interconverting conformers, one of which crystallized. The second new compound, $Fe(C_5H_3)_2$-1,1′-S_3-3,3′-C_3H_6, is shown to exist as four conformers that differ in terms of the orientation of the trisulfido and the trimethylene linker groups.

Introduction

The stereochemistry of ferrocenes is fascinating due to the numerous possible substitution patterns. Research on this topic has led to new generations of asymmetric catalysts[1] and organometallic polymers.[2] There has long been interest in the *ansa*-ferrocenes, i.e., those ferrocenes having the two cyclopentadienyl rings linked by straps of various lengths.[3] The strap typically consists of one to four atoms. Several cases exist with multiple straps between the rings, e.g., the series $Fe(C_5H_{5-n})_2(C_xH_{2x})_n$[4] and the recently described $Fe(C_5H_3)_2(S_3)_2$.[5] We are not, however, aware of examples where the cyclopentadienyl rings are linked via two different straps. In the course of our research on ferrocene trisulfides[6] (also known as trithiaferrocenophanes), we have prepared two examples of doubly *ansa* derivatives. Although the synthetic routes are inefficient, the structures and conformational dynamics of the products are noteworthy.

There were two issues we wished to examine with the new compounds. First, we wanted to elucidate the importance of freely rotating Cp rings in the ring-opening polymerization leading to poly(ferrocenylenepersulfide)s (eq 1). Unfortunately, the solubility of the new complexes is not high enough for us to definitively answer this question. Poly(ferrocenylenepersulfide)s are soluble only when substituted with alkyl chains.[6]

$$\text{(1)}$$
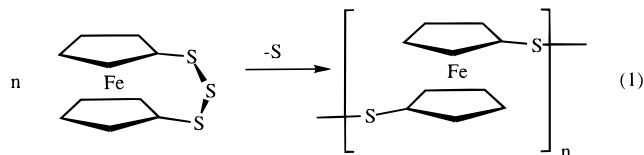
A second issue relevant to this work concerns the mechanism of the refolding of the trisulfido strap in $Fe(C_5H_4)_2S_3$ and analogous compounds (eq 2). It has been

$$\text{(2)}$$
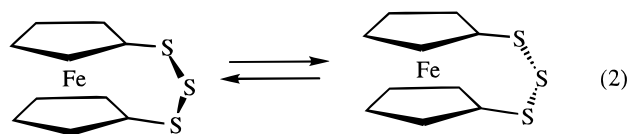
suggested that the conformers of $Fe(C_5H_4)_2S_3$ interconvert via rotation of one cyclopentadienyl ring to a staggered rotamer.[7] The staggered rotamer, with C_2 symmetry, could relax from this transition state by rotation of one Cp ring in either of the two directions, thus reforming the two stable rotamers with equal probability (Scheme 1). The rotation of the cyclopentadienyl rings in C_2R_4-linked ferrocenes is highly restricted, and the staggered conformation is not easily accessed. Thus, the observation of ring flipping in $Fe(C_5H_3)_2$-1,1′-C_2Me_4-3,3′-S_3 might proceed via a previously unexpected mechanisms.

Results and Discussion

In the following paragraphs, *fc* is used as an abbreviation for two different fragments, $Fe(C_5H_3)_2$ and $Fe(C_5H_4)_2$, which are linked to two and four radicals, respectively.

$Me_4C_2fcS_3$. This compound was prepared starting with the ferrocenophane where the cyclopentadienyl

(1) *Ferrocenes*; Togni, A. Hayashi, T., Eds.; VCH: Weinheim, Germany, 1995.

(2) Manners, I. *Angew. Chem., Int. Ed. Engl.* **1996**, *35*, 1602.

(3) For an excellent review of the early work on *ansa*-ferrocenes, see: Watts, W. E. *Organomet. Chem. Rev.* **1967**, *2*, 231.

(4) Kerber, R. C. In *Comprehensive Organometallic Chemistry*; Wilkinson, G., Stone, F. G. A., Abel, E. W., Eds.; Pergamon: Oxford, 1995; pp 189−91.

(5) Long, N. J.; Sharkey, S. J.; Hursthouse, M. A.; Mazid, M. A. *J. Chem. Soc., Dalton Trans.* **1993**, 23. Galloway, C. P.; Rauchfuss, T. B. *Angew. Chem., Int. Ed. Engl.* **1993**, *32*, 1319.

(6) (a) Compton, D. L.; Rauchfuss, T. B. *Organometallics* **1994**, *13*, 4367. (b) Compton, D. L.; Brandt, P. F.; Rauchfuss, T. B.; Rosenbaum, D. F.; Zukoski, C. F. *Chem. Mater.* **1995**, *7*, 2342.

(7) Abel, E. W.; Bhargava, S. K.; Orrell, K. G. *Prog. Inorg. Chem.* **1984**, *32*, 1.

Scheme 1
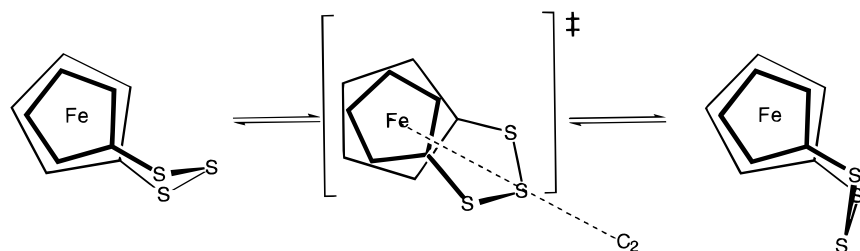
groups are bridged by C_2Me_4. The ferrocene was obtained in a one-pot reaction starting with the reaction of dimethylfulvene with calcium amalgam to give $Me_4C_2C_{10}H_8Ca$,[8] which was treated in situ with $FeCl_2$ to give Me_4C_2fc in 25% yield.[9] Metalation of Me_4C_2fc with 2 equiv of *n*-BuLi·TMEDA followed by treatment with S_8 afforded $Me_4C_2fcS_3$ (**1**) in ∼5% yield (eq 3).

$$(\textbf{1})$$
$$+ \ ..... \quad (3)$$
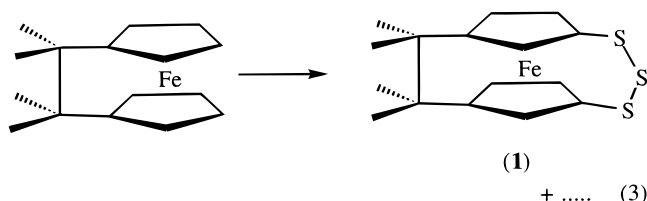
Attempts to improve the yields using other metalating agents such as *t*-BuLi and *n*-BuLi/*t*-BuOK were unsuccessful.

Compound **1** was characterized by elemental analysis, ^{1}H NMR spectroscopy, EI mass spectroscopy, and single-crystal X-ray diffraction. Before discussing the ^{1}H NMR data, it is helpful to first review the results of a single-crystal X-ray diffraction experiment. The Me_4C_2 and S_3 straps are affixed to the cyclopentadienyl rings via 1,1′-3,3′ connectivity (Figure 1). The structural parameters associated with the hydrocarbon portion of **1** are very similar to those for the parent Me_4C_2fc (Table 1).[10] The two cyclopentadienyl rings form a tilt angle of 20.21(3)°. The tilt angle is clearly enforced by the C_2-Me_4 strap since in ferrocene trisulfides the cyclopentadienyl units are almost coplanar, e.g. 4.44(4)° for (*t*-Bu)$_2fcS_3$.[6] Structural analogues of Me_4C_2fc such as $(C_5H_4)_2FeSi_2Me_4$ and $(C_5H_4)_2FeSiMe_2$ have been reported[11] to adopt tilt angles of 4.19(2)° and 20.8(5)°, respectively. Within the FeC_{10} core of **1**, the Fe–C distances range from 1.960(8) to 2.048(7) Å. As seen in Me_4C_2fc,[10] the shortest Fe–C distances are associated with the carbon atoms, C3 and C8, in this case, that are connected to the ethylene bridge. The C–C distances within the cyclopentadienyl rings range from 1.413(7) to 1.433(7) Å vs 1.401 to 1.450 Å seen in $Me_4C_2fcS_3$. Solution NMR measurements show, however, that the conformer that crystallizes (see below) is

(8) Rieckhoff, M.; Pieper, U.; Stalke, D.; Edelmann, F. T. *Angew. Chem., Int. Ed. Engl.* **1993**, *32*, 1079.
(9) Efforts to produce highly soluble *ansa*-ferrocenes prompted us to investigate the synthesis of Et_4C_2fc and $(C_6H_{10})_2C_2fc$. We were able to prepare fulvenes by condensation of C_5H_6 and diethyl ketone and cyclohexanone, respectively, but conversion of these species to ferrocene derivatives was only successful in the cyclohexanone case. Unfortunately, $(C_6H_{10})_2C_2fc$ does not exhibit good solubility characteristics: Compton, D. L. Ph.D. Thesis, University of Illinois at Urbana–Champaign, 1996.
(10) Laing, M. B.; Trueblood, K. N. *Acta Crystallogr.* **1965**, *19*, 373.
(11) Finckh, W.; Tang, B.-Z.; Foucher, D. A.; Zamble, D. B.; Ziembinski, R.; Lough, A.; Manners, I. *Organometallics* **1993**, *12*, 823.

Table 1. Selected Bond Distances (Å) and Angles (deg) for 1,1′-3,3′-Me$_4$C$_2$*fc*S$_3$ (1)

Fe–C1	2.036(8)	C1–S1	1.754(6)	C8–C9	1.424(7)
Fe–C2	2.002(6)	C6–S3	1.767(5)	C9–C10	1.428(7)
Fe–C3	1.972(6)	S1–S2	2.067(8)	C6–C10	1.415(8)
Fe–C4	2.025(8)	S2–S3	2.057(4)	C3–C11	1.545(7)
Fe–C5	2.050(10)	C1–C2	1.438(7)	C8–C14	1.541(8)
Fe–C6	2.028(8)	C2–C3	1.443(7)	C11–C12	1.537(8)
Fe–C7	2.008(8)	C3–C4	1.438(7)	C11–C13	1.537(8)
Fe–C8	1.960(8)	C4–C5	1.413(7)	C14–C15	1.534(8)
Fe–C9	2.020(7)	C1–C5	1.420(8)	C14–C16	1.537(8)
Fe–C10	2.048(7)	C6–C7	1.416(7)	C11–C14	1.613(10)
		C7–C8	1.433(7)		

S1–S2–S3	108.3(2)	C1–S1–S2	103.7(2)	C6–S3–S2	102.2(2)
C8–C14–C11	110.0(4)	C3–C11–C14	109.7(4)	tilt angle[a]	20.21(3)

[a] The tilt angle is defined as the angle formed by the intersection of the planes of the cyclopentadienyl rings.
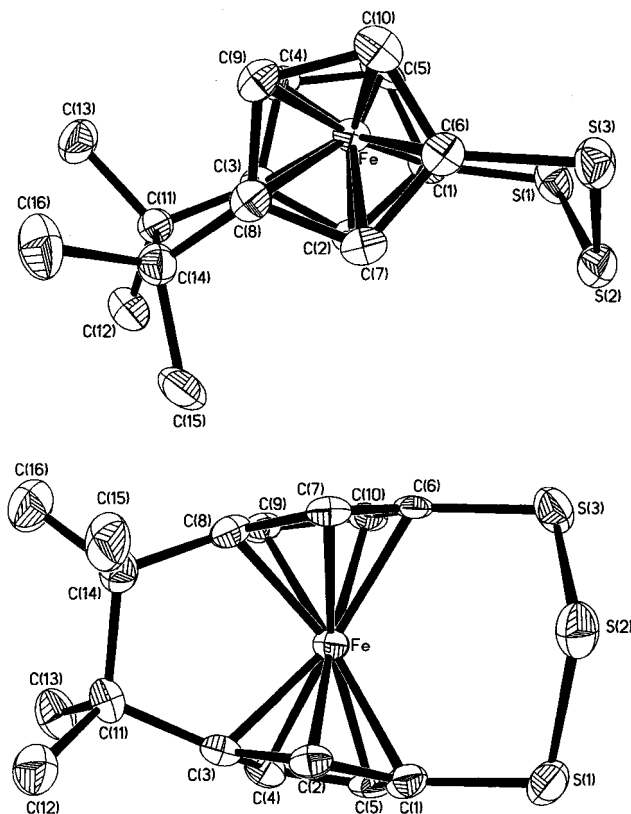

Figure 1. Two views of the nonhydrogen atoms in $Me_4C_2fcS_3$ (**1**), with thermal ellipsoids drawn at the 25% probability level.

only slightly more stable that the one that positions S2 away from the hydrocarbon strap. It is clear from Figure 1 that the observed conformation is not influenced by steric effects since S2 is distant from the C_2-Me_4 strap. The angle associated with S1–S2–S3 is 108.3(2)° vs 103.7(1)° for (*t*-Bu)$_2fcS_3$[6] and 103.9(2)° for fcS_3.[12] Divalent sulfur typically adopts 90° angles.

On the basis of the crystallographic results, the ^{1}H NMR spectrum of Me$_4$C$_2$fcS$_3$ was expected to consist of one pair of methyl singlets and three C$_5$H$_3$ signals. Instead we observed twice the numbers of signals. Both of the two subspectra are appropriate for the solid-state structure of Me$_4$C$_2$fcS$_3$. The disparity between the ^{1}H NMR and crystallographic results was reconciled upon finding that the ^{1}H NMR spectrum depended on the time interval between sample preparation (i.e., dissolution in the solvent) and the recording of the spectrum. The ^{1}H NMR spectrum of freshly prepared solutions of Me$_4$C$_2$fcS$_3$ are enriched in one of the two conformers, as indicated by the relative intensities of the two subspectra observed in equilibrated samples. We conclude that Me$_4$C$_2$fcS$_3$ is subject to a slow conformational equilibrium whose activation barrier exceeds that observable by variable-temperature ^{1}H NMR measurements but which is low enough that isomerization occurs in minutes at room temperature in solution (eq 4). The
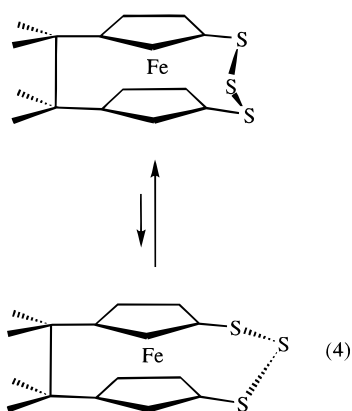
approach to equilibrium followed first-order kinetics, k = 0.0016 s^{-1}. At ambient temperature in CH$_2$Cl$_2$ solution, the equilibrium constant is 3 ± 0.3, favoring the isomer shown in Figure 1. The ^{1}H NMR spectrum was invariant from 20 to 100 °C.

1,1′,3,3′-Trimethyleneferrocene Trisulfide. The second *ansa*-ferrocene investigated in this work features trimethylene and trisulfido straps. Metalation of C$_3$H$_6$fc[13] with 2 equiv of *n*-BuLi·TMEDA followed by treatment with S$_8$ gave an 8% yield of C$_3$H$_6$fcS$_3$ (**2**), which was purified by column chromatography. The mass spectrum and the microanalytical data support this formulation (eq 5). The ^{1}H NMR spectroscopy of **2**,
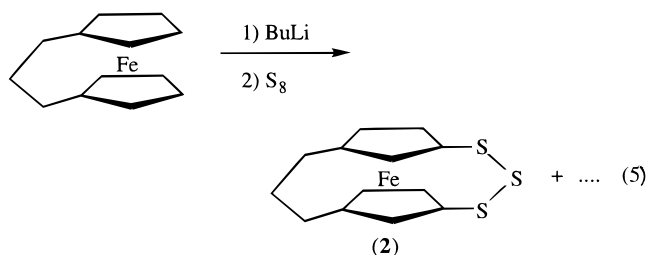
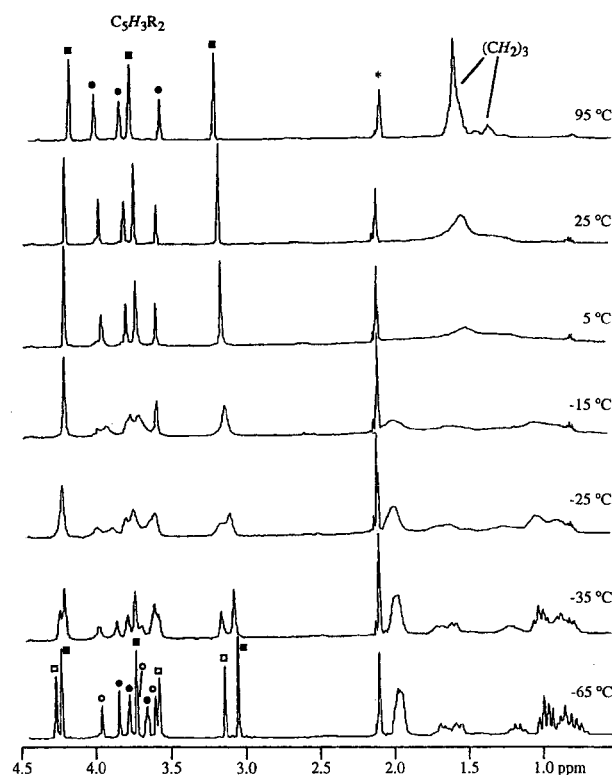while complex, can be assigned in a self-consistent manner with the assumption that the S$_3$ and (CH$_2$)$_3$

(12) Davis, B. R.; Bernal, I. *J. Cryst. Mol. Struct.* **1972**, *2*, 107.
(13) The metalation of [3]ferrocenophane has been studied previously, see: Talham, D. R.; Cowan, D. O. *Organometallics* **1987**, *6*, 932. Hillman, M.; Matyevich, L.; Jagwani, W.; McGowan, J. *Organometallics* **1982**, *1*, 1226.

Figure 2. 400 MHz ^{1}H NMR spectra of a C$_6$D$_5$CD$_3$ solution of C$_3$H$_6$fcS$_3$ (**2**) at various temperatures. The circles and squares in the high-temperature spectrum indicate the C$_5$H$_3$ signals of the two conformers that differ in terms of the orientation of the trisulfido strap. The open and filled circles and squares in the low-temperature spectrum distinguish C$_5$H$_3$ signals for conformers that differ in terms of the relative orientation of the trimethylene strap (see Scheme 2).

straps are in the 1,1′ and 3,3′ positions. Variable-temperature NMR measurements revealed a dynamic process with a low activation energy (~40 kJ/mol), Figure 2. Line broadening is due to the fact that the "refolding" of the (CH$_2$)$_3$ strap occurs on the ^{1}H NMR time scale. Consistent with the findings on **1**, the refolding of the S$_3$ strap in **2** is subject to a much higher barrier. The main observations are as follows: (i) At −65 °C, the ^{1}H NMR spectrum features 11 of the 12 expected C$_5$H$_3$R$_2$ resonances, six being ~50% more intense than the others. The methylene groups appear as a series of partially resolved multiplets in the region δ 2.0−0.5. (ii) A low-temperature (−90 °C) two-dimensional ^{1}H−^{1}H COSY NMR analysis of the C$_5$H$_3$ region confirmed the presence of four subspectra, each associated with three C$_5$H$_3$R$_2$ signals. (iii) At 25 °C, the refolding of the (CH$_2$)$_3$ bridge is rapid on the NMR time scale, as seen for other (CH$_2$)$_3$-strapped ferrocenes.[12] The spectrum features six C$_5$H$_3$R$_2$ resonances, while the CH$_2$ signals are very broad. The simplification of the C$_5$H$_3$ signals results from the coalescence of intense signals with other intense signals as well as the coalescence of less intense signals with the other less intense signals. This behavior indicates that the high activation barrier process corresponds to K_{eq}[b] in Scheme 2. (iv) The six C$_5$H$_3$R$_2$ signals remain unchanged over the range 25−95 °C. The increased rate of refolding of the (CH$_2$)$_3$
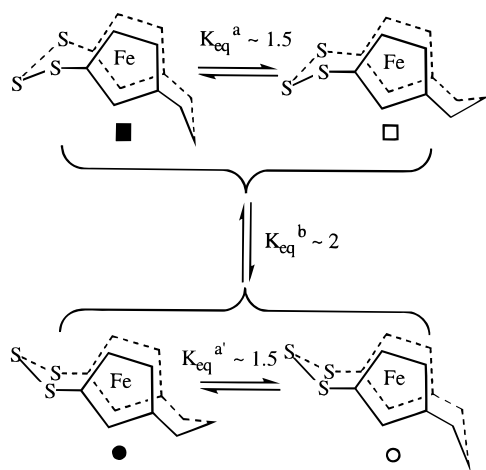
Scheme 2

strap over this temperature interval is, however, manifested by the sharpening of the CH_2 multiplets at δ 1.58 and 1.35.

The processes in Scheme 2 are proposed to explain these data. It is, however, unclear as to which orientations the $(CH_2)_3$ and S_3 straps are energetically preferred.

Summary

In this work, we have identified two novel double *ansa*-ferrocenes. These species display conformational equilibria which provide new insights into the dynamics of this class of compounds.

Perhaps the more interesting of the two compounds is the C_2Me_4-bridged species **1**. We were able to monitor its isomerization starting from the conformer that happens to crystallize more readily. Our results are usefully interpreted in the context of the related double *ansa*-ferrocene Fe(4-Bu^{t}C$_5$H$_2$)(4-Bu^{t}C$_5$H$_3$)-1,1'-S$_3$-2,2'-S$_3$,[5] whose isomerization is only $\sim$5 times more rapid than for **1**, i.e., $k_1 \approx k_{-1} \approx 5 \times 10^{-4}$ s^{-1} (18 °C) for $\Delta G^{\ddagger}$ = 91 kJ/mol.[14] In the present study, we have further constrained the rotational mobility of the cyclopentadienyl rings. Obviously, this does not strongly inhibit the refolding dynamics of the trisulfido strap. This finding is not in agreement with the previously suggested[7] mechanism for this isomerization process.

Experimental Section

Materials and Methods. Schlenk techniques were employed throughout. Granular calcium and zinc powder were purchased from Aldrich and Cerac, respectively. Otherwise, the experimental and spectroscopic protocols were as previously described.[6b]

Me$_4$C$_2$C$_{10}$H$_8$Ca. This procedure was adapted from that of Rieckhoff et al.[6] A suspension of 10.0 g (0.250 mol) of Ca and 1.00 g of HgCl$_2$ in 500 mL of THF was allowed to stand for 18 h and then stirred vigorously for 5 h. This slurry was cooled in an ice bath and treated with 26.85 g (0.252 mol) of 6,6-dimethylfulvene. The cloudy pale yellow slurry was allowed to warm to room temperature and then stirred for 16 h. The slurry was filtered via cannula, and the remaining gray solid was washed with two 50 mL portions of THF. The solvent was removed from the cloudy green-yellow filtrate, and the

residue was dried at 100 °C under vacuum for 2 h to give a brittle, glassy, yellow-brown solid. The Me$_4$C$_2$C$_{10}$H$_8$Ca was used in the next step without further purification. Yield: 33.4 g (26% based on 6,6-dimethylfulvene).

Me$_4$C$_2$*fc*. A slurry of 33.44 g (0.132 mol) of Me$_4$C$_2$C$_{10}$H$_8$Ca and 12.45 g (0.098 mol) of FeCl$_2$ in 500 mL of THF was heated at reflux for 18 h. The reaction mixture was diluted with 500 mL of hexane, and the resulting brown-orange slurry was filtered through a 10 × 5 cm bed of silica gel. The silica gel was washed with four 50 mL portions of hexane. The combined filtrates were evaporated to give a red-orange solid. The solid was recrystallized by dissolution in 100 mL of boiling hexane followed by cooling to −23 °C. The resulting red-orange crystals were filtered off, washed with two 10 mL portions of cold hexane, dried in vacuo, and sublimed (45 °C, 0.3 Torr). Yield: 7.4 g (28% based on FeCl$_2$). ^{1}H NMR (C$_6$D$_6$): δ 4.50 (m, 4H), 3.99 (m, 4H), 1.11 (s, 12H).

Me$_4$C$_2$*fc*S$_3$ (1). A Schlenk flask was charged with 1.0382 g (3.87 mmol) of Me$_4$C$_2$*fc* and 50 mL of hexanes. The resulting orange solution was treated with 5.0 mL of BuLi, 1.6 M solution in hexanes (8.0 mmol), followed by 1.2 mL (8.0 mmol) of TMEDA. After 60 h, the dark red solution was treated with 1.25 g of S$_8$ (39 mmol), resulting in a mildly exothermic process and a color change to orange-brown. After stirring for 7 days (probably not needed), the solution was filtered through a bed of Celite which was washed with Et$_2$O, hexanes, and finally benzene. The combined extracts were evaporated. The extract was further purified by chromatography on a 25 mm column of silica gel, eluting with hexanes (subsequent elution with benzene gave Me$_4$C$_2$*fc*S$_3$ together with Me$_4$C$_2$*fc*S$_n$, where n = 4 and 5). The hexane fraction, which, based on NMR analysis, contained Me$_4$C$_2$*fc*H, Me$_4$C$_2$*fc*S$_3$, and an unknown compound, was rechromatographed on a 15 cm column of silica gel to give analytically pure Me$_4$C$_2$*fc*S$_3$. Yield: 0.14 g (10%). Anal. Calcd for C$_{16}$H$_{18}$FeS$_3$: C, 53.03; H, 5.01; Fe, 15.41; S, 26.55. Found: C, 52.80; H, 4.86; Fe, 15.57; S, 26.49. Although the sample was analytically pure, its ^{1}H NMR spectrum exhibited an impurity that was removed by treatment of the reaction mixture at −78 °C with 0.33 equiv of Bu$_3$P. This solution was allowed to warm to 25 °C, and after 1 h, the solution was evaporated and chromatographed on a column of silica gel eluting with hexanes. This was recrystallized from hot hexanes. ^{1}H NMR (C$_6$D$_6$): major isomer δ 4.33 (d of d, J = 1.6, 0.7 Hz, 2H), 4.27 (d of d, J = 1.2, 1.0 Hz, 2H), 3.85 (t, J = 1.2 Hz, 2H), 0.91 (s, 6H), 0.73 (s, 6H); minor isomer δ 4.75 (t, J = 1.2 Hz, 2H), 4.36 (d of d, J = 1.6, 0.7 Hz, 2H), 3.74 (d of d, J = 1.2, 1.2 Hz, 2H), 0.87 (s, 6H), 0.77 (s, 6H). ^{13}C{^{1}H} NMR (C$_6$D$_6$): δ 98.5, 96.0, 92.6, 87.6, 84.7, 81.8, 75.7, 74.2, 73.0, 71.8, 57.8 (impurity), 50.2, 49.0, 27.4, 27.3, 26.8, 26.7. UV−vis (CH$_2$Cl$_2$): 236, 282 (sh), 396 nm. EIMS (70 eV) calcd for C$_{16}$H$_{18}$FeS$_3$ 361.992005 (found 361.991880). FD MS: 362 (100, M$^+$). Cyclic voltammetry (CH$_2$Cl$_2$, Bu$_4$NPF$_6$): 786 mV vs Ag/AgCl (reversible).

A solution of **1** in C$_6$D$_6$ was prepared in a 5 mm NMR tube. The progress of the isomerization was monitored by ^{1}H NMR spectroscopy. Plots of ln[%initial isomer] vs time were linear. The rate constant for isomerization of the major isomer to the smaller one is 0.0016 s^{-1} (the kinetics were measured at the NMR probe temperature, $\sim$27 °C).

C$_3$H$_6$*fc*S$_3$ (2). C$_3$H$_6$*fc* was prepared in 12% yield by an adaptation of Dormond and Weed's procedures[15,16] in a one-pot reaction starting with the alkylation of LiC$_5$H$_5$ with Br(CH$_2$)$_3$Br followed by BuLi and finally FeCl$_2$. A solution of 0.2517 g (1.11 mmol) of C$_3$H$_6$*fc* in 30 mL of hexane was treated with 1.40 mL (2.23 mmol) of a 1.6 M hexane solution of BuLi followed by 0.34 mL (2.23 mmol) of TMEDA. After 24 h, the

(14) Rauchfuss, T. B.; Galloway, C. P. *Phosphorus, Sulfur, Silicon* **1994**, *93*, 117.

(15) Lüttringhaus, A.; Kullick, W. *Angew. Chem.* **1958**, *70*, 438.
(16) Dormond, A.; Ou-Khan; Tirouflet, J. *J. Organomet. Chem.* **1976**, *110*, 321. Weed, J. T.; Rettig, M. F.; Wing, R. M. *J. Am. Chem. Soc.* **1983**, *105*, 6510.

Table 2.   Crystal Data and Structure Refinement for 1

empirical formula	$C_{16}H_{18}FeS_3$
fw	362.33
temperature	198(2) K
wavelength	0.710 73 Å
cryst syst	monoclinic
space group	$P2_1/n$
unit cell dimens	$a = 6.88(3)$ Å
	$b = 11.023(3)$ Å
	$c = 19.682(5)$ Å
	$V = 1485(7)$ Å^3
	$\alpha = 90°$
	$\beta = 95.82(3)°$
	$\gamma = 90°$
	$Z = 4$
density (calcd)	1.621 Mg/m^3
abs coeff	1.423 mm^{-1}
cryst size	$0.32 \times 0.10 \times 0.10$ mm
θ range for data collection	2.08–23.97°
index ranges	$0 \le h \le 7$, $-12 \le k \le 0$,
	$-22 \le 1 \le 22$
collection method	$\omega–\theta$ scan profiles
no. of reflns collected	2540 ($R_{int} = 0.0431$)
indep reflns	2325 (1522 obsd, $I > 2\sigma(I)$)
refinement (shift/err = 0.001)	full-matrix least-squares on F^2
data/restraints/params	2324/0/181
goodness-of-fit on F^2	1.055
final R indices (obsd data)^a	$R_1 = 0.0463$, $wR_2 = 0.0881$
R indices (all data)	$R_1 = 0.1084$, $wR_2 = 0.1102$
largest diff peak and hole	0.414 and -0.330 e Å^{-3}

solution had changed colors from orange to dark red. The solution was cooled to 0 °C and treated with 0.36 g (11 mmol) of S_8. The slurry was heated at 50 °C for 24 h. The now dark brown-red slurry was filtered through a 2×3 cm bed of Celite, and the Celite was washed with three 10 mL portions of hexane. The orange filtrate was washed with two 25 mL portions of 10% aqueous NaOH, dried over Na_2SO_4, reduced to ca. 30 mL, and chromatographed on a 30×3 cm column of silica gel, eluting with hexane. The first, light yellow band was shown by ^1H NMR spectroscopy to be C_3H_6fc. The second, orange band proved to be the desired product. Yield: 0.0285 g (8% based on C_3H_6fc). Anal. Calcd for $C_{18}H_{24}FeS_3$: C, 48.75; H, 3.78; Fe, 17.43; S, 30.00. Found: C, 48.69; H, 4.06; Fe, 16.98; S, 30.39. ^1H NMR (C_6D_6, integrations are approximate since there are two isomers): δ 4.25 (s, 2H), 4.05 (s, 1H), 3.81 (s, 1H), 3.72 (s, 2H), 3.63 (s, 1H), 3.21 (s, 2H), 1.3 (br s, 9H). EI MS (70 eV): 320 (M$^+$).

Crystallographic Study of Me$_4$C$_2$*fc*S$_3$ (1). The crystal was grown by slowly cooling a solution of 10 mg of **1** in 1 mL of hexane. Using Paratone oil, the crystal was affixed to a glass fiber with the (2 −1 2) plane approximately normal to the spindle axis. The data crystal was bound by the (0 1 −1), (0 −1 1), (0 1 0), (0 −1 −1), (−1 1 −1), and (1 0 0) faces. Distances from the crystal center to these facial boundaries were 0.05, 0.05, 0.05, 0.05, 0.16, and 0.16 mm, respectively. Data were measured at 198 K on an Enraf-Nonius CAD4 diffractometer. Crystal and refinement details are given in the Supporting Information. Systematic conditions suggested the space group $P2_1/n$. Three standard intensities monitored every 90 min showed no decay of the sample. Step-scanned intensity data were reduced by profile analysis and corrected for Lorentz and polarization effects. Empirical absorption corrections, SHELX-76, were applied using SHELXTL 5.03. Scattering factors and anomalous dispersion terms were taken from standard tables.

The structure was solved by direct methods using SHELX 90; correct positions for Fe and S atoms were deduced from an *E*-map. One cycle of isotropic least-squares refinement followed by an unweighted difference Fourier synthesis revealed positions for non-H atoms. Methyl H atom positions, R–CH$_3$, were optimized by rotation about R–C bonds with idealized C–H, R–H, and H···H distances. Remaining H atoms were included as fixed idealized contributors. H atom U's were assigned as 1.2 times U_{eq} of adjacent non-H atoms. Non-H atoms were refined with anisotropic thermal coefficients. Successful convergence of the full-matrix least-squares refinement on F^2 was indicated by the maximum shift/ error for the last cycle. The highest peak in the final difference Fourier map was in the vicinity of the Fe and sulfur atoms; the final map had no other significant features. The details of the data collection and refinement are collected in Table 2.

Supporting Information Available: Tables of thermal parameters, crystal and data collection details, and atomic coordinates (11 pages). Ordering information is given on any current masthead page.